

## LETTER TO THE EDITOR

## Coherently tunable third-order nonlinearity in a nanojunction

Vadim A Markel

Departments of Radiology and Bioengineering, University of Pennsylvania, Philadelphia, PA 19104, USA

E-mail: [vmarkel@mail.med.upenn.edu](mailto:vmarkel@mail.med.upenn.edu)

Received 19 July 2005, in final form 20 September 2005

Published 11 October 2005

Online at [stacks.iop.org/JPhysB/38/L347](http://stacks.iop.org/JPhysB/38/L347)

### Abstract

A possibility of tuning the phase of the third-order Kerr-type nonlinear susceptibility in a system consisting of two interacting metal nanospheres and a nonlinearly polarizable molecule is investigated theoretically and numerically. It is shown that by varying the relative inter-sphere separation, it is possible to tune the phase of the effective nonlinear susceptibility  $\chi^{(3)}(\omega; \omega, \omega, -\omega)$  in the whole range from 0 to  $2\pi$ .

Optical and, more generally, electromagnetic properties of nanostructures have been of great interest in the past decade [1–5]. In particular, physical effects due to the local field enhancement have recently attracted significant attention [5–8]. In this respect, nanoparticles of noble metals, especially silver, proved to be very useful. Recent dramatic advances in nanofabrication made it possible to design, arrange and assemble such nanoparticles with great precision. The remarkable optical properties of silver nanostructures are explained by the strong, resonant interaction with electromagnetic fields in the visible and near-IR spectral range and by very small Ohmic losses.

The strong enhancement of local fields in small spatial areas is a consequence of two factors: the heterogeneity of a nanostructure on a subwavelength scale and the resonant character of interaction of the electromagnetic field with the nanostructure. Both features are, in principle, present even in the case of a single isolated nanosphere. However, the effect becomes much stronger in aggregated nanospheres due to the effect of *plasmon hybridization* [9]. In this case, amplification of the local field can become sufficiently large to make possible detection of Raman radiation from a single molecule, as was demonstrated experimentally in [10]. The Raman enhancement factor  $(|\mathbf{E}|/|\mathbf{E}_0|)^4$  in the centre of a junction between two nanospheres ( $\mathbf{E}$  and  $\mathbf{E}_0$ —the local and the external fields in the junction, respectively) was calculated to be  $5.5 \times 10^9$  for a 1 nm gap between two silver spheres of 60 nm radius each at  $\lambda = 497$  nm [11]. Even larger enhancement, up to  $10^{13}$ , was predicted in the so-called nanolens—a linear chain of several nanospheres of different sizes [6].

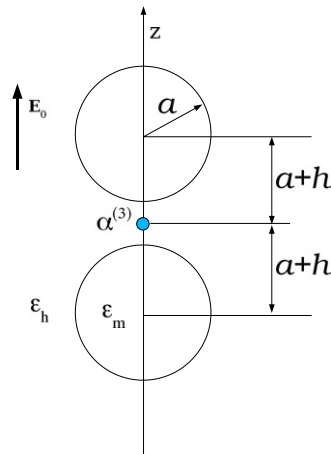


**Figure 1.** Schematic illustration of the physical system considered in this letter.

The primary focus of research in single-molecule spectroscopy has been on non-coherent optical processes such as Raman scattering. In this letter, I consider a coherent nonlinear effect, namely, degenerate third-order nonlinearity, and demonstrate that, by changing the geometry of a nanostructure, it is possible to control not only the amplitude of a nonlinear response but also its phase (relative to the phase of the incident field). The optical Kerr effect described by the third-order susceptibility  $\chi^{(3)}(\omega; \omega, \omega, -\omega)$  gives rise to nonlinear corrections to absorption and refraction indices. The ability to control the phase and tensor structure of  $\chi^{(3)}$  can have numerous applications. For example, in quantum non-demolition measurements via the optical Kerr effect, it is typically assumed that the nonlinear refractive index  $n_2$  is purely positive (although this assumption is usually not stated explicitly) [12–14]. However, most nonlinear molecules with relatively large values of third-order polarizability exhibit both nonlinear refraction and nonlinear absorption. For example, the figure of merit  $T = \beta\lambda/\text{Re}(n_2)$  ( $\beta = 2\pi \text{Im}(n_2)$  being the two-photon absorption coefficient) of ultrafast third-order optical nonlinearity of a conjugated 3,3'-bipyridine derivative was measured to be 1.05 and 1.59 at  $\lambda = 750$  nm and  $\lambda = 1200$  nm, respectively [15]. (The value of  $T$  smaller than unity was obtained in this work at a somewhat larger wavelength,  $\lambda = 1550$  nm.) The effect described in this letter would allow one to make  $T$  arbitrarily small in a certain range of wavelengths, typically, in the visible and near-IR. Apart from applications in quantum optics, this may be very important in telecommunications, in particular, for development of all-optical switches based on the third-order nonlinearity [16].

Note that in this letter the microscopic mechanism for the molecular nonlinear polarizability is not discussed and the latter is introduced through a phenomenological parameter. The main point of this letter is to show that, regardless of the actual value of the complex molecular polarizability  $\alpha^{(3)}$ , it is possible to incorporate the nonlinear molecule in a metal nanosystem in such a way that the *effective* nonlinear polarizability  $\alpha_{\text{eff}}^{(3)}$  would have any given phase. In particular, the phase of  $\alpha_{\text{eff}}^{(3)}$  can be tuned to be exactly zero, which would correspond to  $T_{\text{eff}} = 0$ .

Consider a simple physical system shown schematically in figure 1. Here a nonlinearly-polarizable molecule is placed in the centre of symmetry of two spheres. The radius of each sphere is denoted by  $a$  and the width of the gap (surface-to-surface) by  $2h$ . Thus, for example, if  $a = 50$  nm and  $2h = 1$  nm, which is the smallest physical gap considered in [11], we have

$h/a = 0.01$ . The system is excited by a monochromatic incident wave with the frequency  $\omega$  and wavelength in vacuum  $\lambda = 2\pi c/\omega$ , linearly polarized along the axis of symmetry. The latter coincides with the  $z$ -axis. The whole system is assumed to be sufficiently small compared to  $\lambda$  and we work in the quasistatic approximation. Further, we use the Drude formula for the dielectric function of metal, namely,

$$\varepsilon = \varepsilon_0 - \omega_p^2 / \omega(\omega + i\gamma). \quad (1)$$

The following parameters are used in the simulations:  $\varepsilon_0 = 5$ ,  $\gamma/\omega_p = 0.002$ , and the value of  $\omega_p$  is unspecified. Note that the dielectric function of silver in the anomalous dispersion region is well described by choosing  $\omega_p \approx 4.6 \text{ s}^{-1}$  ( $\lambda_p \approx 136 \text{ nm}$ ). Finally, we assume that the metal nanoparticles are embedded in a transparent host medium with a refractive index of  $n_h = 2$  ( $\varepsilon_h = 4$ ).

Because of the axial symmetry, the dipole moment induced in the molecule is parallel to the  $z$ -axis. The third-order nonlinear correction to the dipole moment oscillating at the same temporal frequency as the incident field is given by

$$d_z^{(NL)}(t) = \alpha^{(3)} E_z |E_z|^2 = \alpha_{\text{eff}}^{(3)} E_0 |E_0|^2 \exp(-i\omega t). \quad (2)$$

Here  $E_z$  is the amplitude of the local electric field at the location of the molecule and  $E_0$  is the amplitude of the incident wave. Note that, even if we assume for simplicity that  $E_0$  is purely real,  $E_z$  can be complex. In general, there can be an arbitrary phase shift between the local and the external fields. The effective nonlinear polarizability  $\alpha_{\text{eff}}^{(3)}$  is related to  $\alpha^{(3)}$  by

$$\alpha_{\text{eff}}^{(3)} = G\alpha^{(3)}, \quad (3)$$

where the enhancement factor  $G$  is given by

$$G = \frac{E_z |E_z|^2}{E_0 |E_0|^2}. \quad (4)$$

Since  $G$  is, in general, complex, it can influence not only the magnitude but also the phase of the effective third-order polarizability. Below, we calculate  $G$  numerically and show that its phase can be varied in its whole range by changing the inter-sphere separation.

To calculate the local field in the gap,  $E_z$ , we expand the polarization inside each sphere in the quasistatic vector spherical harmonics  $\mathbf{X}_{ilm}^{(1)}(\mathbf{r}) = (la)^{-1/2} \nabla \psi_{lm}^{(1)}(\mathbf{r} - \mathbf{r}_i)$ . Here  $i = 1, 2$  indexes the nanospheres,  $\mathbf{r}_i$  are the radius vectors of the spheres' centres,  $\psi_{lm}^{(1)}(\mathbf{r}) = (r/a)^l Y_{lm}(\hat{\mathbf{r}})$ , and  $Y_{lm}(\hat{\mathbf{r}})$  are spherical functions of the polar angles of the unit vector  $\hat{\mathbf{r}}$ . Polarization inside the  $i$ th sphere can be written as

$$\mathbf{P}(\mathbf{r}) = \sum_{lm} C_{ilm} \mathbf{X}_{ilm}^{(1)}(\mathbf{r}), \quad \text{if } |\mathbf{r} - \mathbf{r}_i| < a, \quad (5)$$

where the unknown coefficients  $C_{ilm}$  must be found from the standard boundary conditions applied at the surface of each sphere, or alternatively, from the integral equation formalism as described in [17]. From general considerations, it is clear that  $C_{ilm}$  obey a system of linear equations which, in the quasistatic limit, was obtained in [18] and simplified in [19]. In general, this set of equations has the form

$$(1/\chi - W)|C\rangle = |E\rangle, \quad (6)$$

where  $\chi = (3/4\pi)[(\varepsilon - \varepsilon_h)/(\varepsilon + 2\varepsilon_h)]$  is the coupling constant,  $W$  is the electromagnetic interaction matrix and  $|E\rangle$  is the appropriate right-hand side defined by the external field. In the case of axial symmetry, only modes with  $m = 0$  are excited, so that  $C_{ilm} = C_{il0}\delta_{m0}$ .

The matrix elements of  $W$  needed to find the solution are

$$\begin{aligned} \langle il0|W|i'l'0\rangle &= \frac{l\delta_{ll'}\delta_{ii'}}{2l+1} + (1-\delta_{ii'})(-1)^l [\text{sgn}(z_i - z_{i'})]^{l+l'} \\ &\times \sqrt{\frac{l!}{(2l+1)(2l'+1)l!l'!(1+h/a)^{l+l'+1}}} \frac{(l+l')!}{(2l+1)(2l'+1)l!l'!(1+h/a)^{l+l'+1}} \end{aligned} \quad (7)$$

and the components of the right-hand side vector in (6) are given by

$$\langle il0|E\rangle = E_0\sqrt{4\pi a^3/3}. \quad (8)$$

In general, once the coefficients  $C_{ilm}$  are found, the scattered field at an arbitrary point  $\mathbf{r}$  in the host medium can be found from

$$\mathbf{E}_s(\mathbf{r}) = -\sum_{ilm} C_{ilm} \frac{4\pi(l-1)}{3(2l+1)} \mathbf{X}_{ilm}^{(2)}(\mathbf{r}), \quad (9)$$

where  $\mathbf{X}_{ilm}^{(2)}(\mathbf{r}) = [(l+1)a]^{-1/2} \nabla \psi_{lm}^{(2)}(\mathbf{r} - \mathbf{r}_i)$  are the quasistatic vector spherical harmonics of the second kind and  $\psi_{lm}^{(2)}(\mathbf{r}) = (a/r)^{l+1} Y_{lm}(\mathbf{r})$ . For the particular problem considered in this letter, the only non-zero terms in series (9) are those with  $m = 0$ . Further simplification is obtained if the electric field is evaluated on the axis of symmetry, in which case

$$\mathbf{E}_{sz}(z) = E_0\sqrt{\frac{4\pi}{a^3}} \sum_n \frac{\langle E|P_n\rangle}{1/\chi - w_n} f_n\left(\frac{z}{h}\right), \quad (10)$$

where

$$f_n(x) = \sum_{l=1}^{\infty} (l+1) \sqrt{\frac{l}{2l+1}} \left\{ \frac{\langle l10|P_n\rangle}{[1+(h/a)(1+x)]^{l+2}} - (-1)^l \frac{\langle 2l0|P_n\rangle}{[1+(h/a)(1-x)]^{l+2}} \right\} \quad (11)$$

and  $|P_n\rangle$  are the eigenvectors of  $W$  with corresponding eigenvalues  $w_n$ . Here  $E_{sz}$  is the  $z$ -component of the scattered field on the axis of symmetry (the  $x$ - and  $y$ -components are zero). The total local field  $E_z$  is a superposition of the incident and scattered fields:

$$E_z = E_0 + E_{sz}. \quad (12)$$

Note that we have used the spectral approach to solving (6). In other words, instead of directly inverting  $1/\chi - W$ , we seek eigenvectors and eigenvalues of  $W$  and then obtain the solution in terms of these quantities for an arbitrary coupling constant  $\chi$ .

The matrix  $W$  is of infinite size and in practical calculations must be truncated. The truncation order  $l_{\max}$  required to obtain an accurate solution depends on the inter-sphere separation. Although, for any separation, there exist an infinite number of modes, most of them are antisymmetric [20, 21] or, equivalently, dark [22]. A dark mode is not coupled to the homogeneous external field because the scalar product  $\langle E|P_n\rangle$  is either exactly zero or very small. Correspondingly, the input of a dark mode to series (10) is negligible. Modes which are not dark are referred to as luminous [22]. For a finite value of  $h$ , there is a finite number of luminous modes and the spectrum of eigenvalues  $w_n$  which correspond to these modes is discrete. However, as  $h$  decreases, the number of luminous modes grows and the intervals between consecutive values of corresponding eigenvalues  $w_n$  approach zero. When the two spheres touch, the spectrum becomes continuous and, strictly speaking, cannot be adequately described at any finite truncation order. However, for practical purposes, the matrix still can be truncated, as long as the resultant discrete density of states approximates the true continuous function with sufficient precision. The latter condition depends on the relaxation in the system and is very difficult to satisfy for silver in the near-IR spectral region due to the very small non-radiative relaxation. In the simulations presented below, the minimum ratio

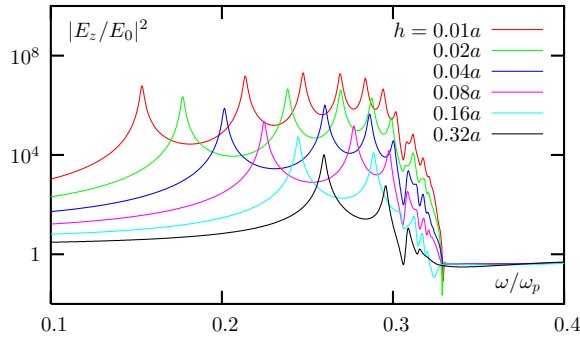


**Figure 2.** The ratio  $|E_z/E_0|^2$  in the centre of the inter-sphere gap as a function of  $\omega/\omega_p$  for different relative inter-sphere separations.

$h/a$  is equal to 0.01. In this case, all luminous modes are obtained with very high precision at relatively modest truncation orders. The results reported below were obtained at  $l_{\max} = 800$  and convergence with machine accuracy was verified by doubling this number.

Now we turn to the numerical results. First, in figure 2, we plot the spectral dependence of the factor  $|E_z/E_0|^2$  in the centre of the inter-sphere gap for different relative separations  $h/a$ . It can be seen that a ‘resonance band’ exists in the spectral region whose bounds depend on the ratio  $h/a$ . For  $h = 0.01a$ , resonance interaction takes place for  $0.15 \lesssim \omega/\omega_p \lesssim 0.33$ . For  $h = 0.32a$ , the resonance band is smaller,  $0.25 \lesssim \omega/\omega_p \lesssim 0.32$ . We will be interested in the frequencies which lie in the resonance band for the smallest value of  $h$  considered, namely,  $h = 0.01a$ .

In figures 3–5, we show the parametric plots of the complex enhancement factor  $G$  for the following values of the ratio  $\omega/\omega_p$ : 0.20, 0.25 and 0.32. In the case  $\omega/\omega_p = 0.20$ , the most dramatic change of  $G$  happens when  $h$  changes from  $0.36a$  to  $0.41a$ . The phase of  $G$  changes in this interval of  $h$  from  $\approx \pi/4$  to  $\approx 3\pi/4$ . Overall, the phase of the enhancement factor can be tuned from  $\approx 0$  to  $\approx \pi$  by tuning  $h$  in the whole considered interval.

Much more control over the phase of  $G$  can be attained for  $\omega/\omega_p = 0.25$ , as shown in figure 4. It is interesting to note that the parametric curve shown in these figure is approximately self-similar, consisting of several almost closed loops which can be seen at different scales. The phase of  $G$  changes in the whole interval from 0 to  $2\pi$ . Qualitatively similar curve was also obtained for  $\omega/\omega_p = 0.30$  (data not shown).

Perhaps, the most interesting curve is obtained at  $\omega/\omega_p = 0.32$  (figure 5), although the magnitude of  $G$  is not as large for this value of  $\omega/\omega_p$  as in figures 3–4. The parametric plot of  $G$  is in this case a spiral. The phase of  $G$  changes monotonically from  $\approx 0$  to  $\approx 5\pi$ . Thus, the curve makes more than two full revolutions around the origin in the complex plane. By varying the parameters in the Drude formula and the refractive index of the host medium, it was found that the spiral shape of the curve is typical when  $\omega/\omega_p$  is close to the right bound of the resonance interaction band (data not shown).

Thus, we have shown that by changing the inter-sphere separation  $h$  from  $0.01a$  to  $0.32a$  it is possible to change the phase of the enhancement factor  $G$ , and, consequently, that of the effective nonlinear polarizability  $\alpha_{\text{eff}}^{(3)}$  in its whole range. Some limitations of the model used in this letter must be mentioned. First, we did not account for direct electromagnetic coupling between the nonlinearly polarizable molecule and the nanospheres, nor did we take into account the nonlinearity of the metal itself. The latter effect can be significant. Further, we assumed purely local dielectric response of the metal and worked in the quasistatic approximation.

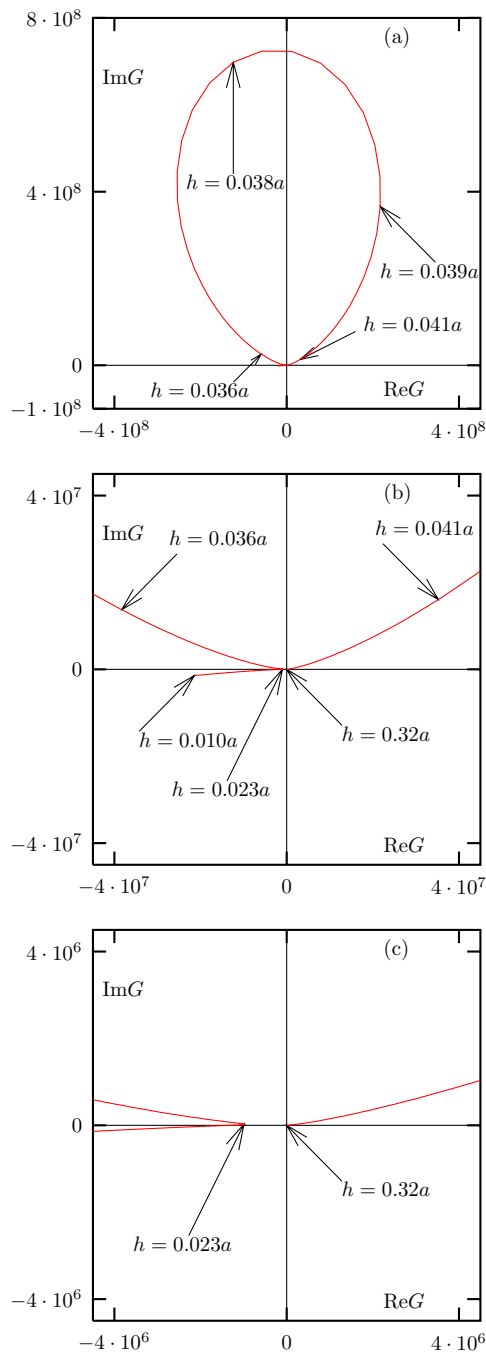


**Figure 3.** The parametric plot of the complex enhancement factor  $G$  as a function of  $h/a$  for  $\omega/\omega_p = 0.2$ . Graphs (a)–(c) show the same curve on different scales.

We did not account for the fact that the electric field in the gap is not constant but can change on the scales comparable to molecular. Although all these factors are important

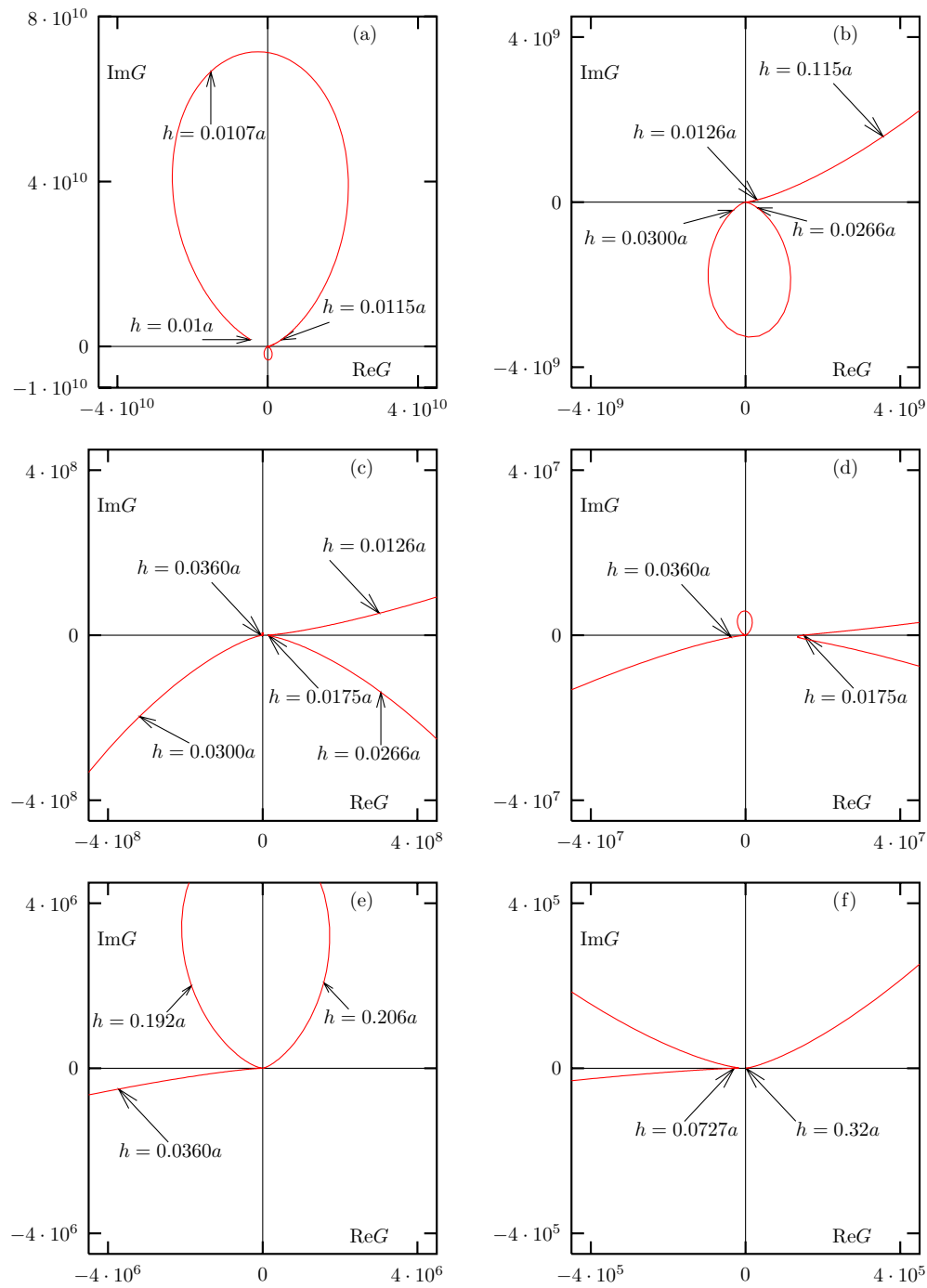


**Figure 4.** Same as in figure 3 but for  $\omega = 0.25\omega_p$ .

if one seeks to calculate the nonlinear response of the system with precision, inclusion of all these complications would make the theoretical description unrealistically complicated.

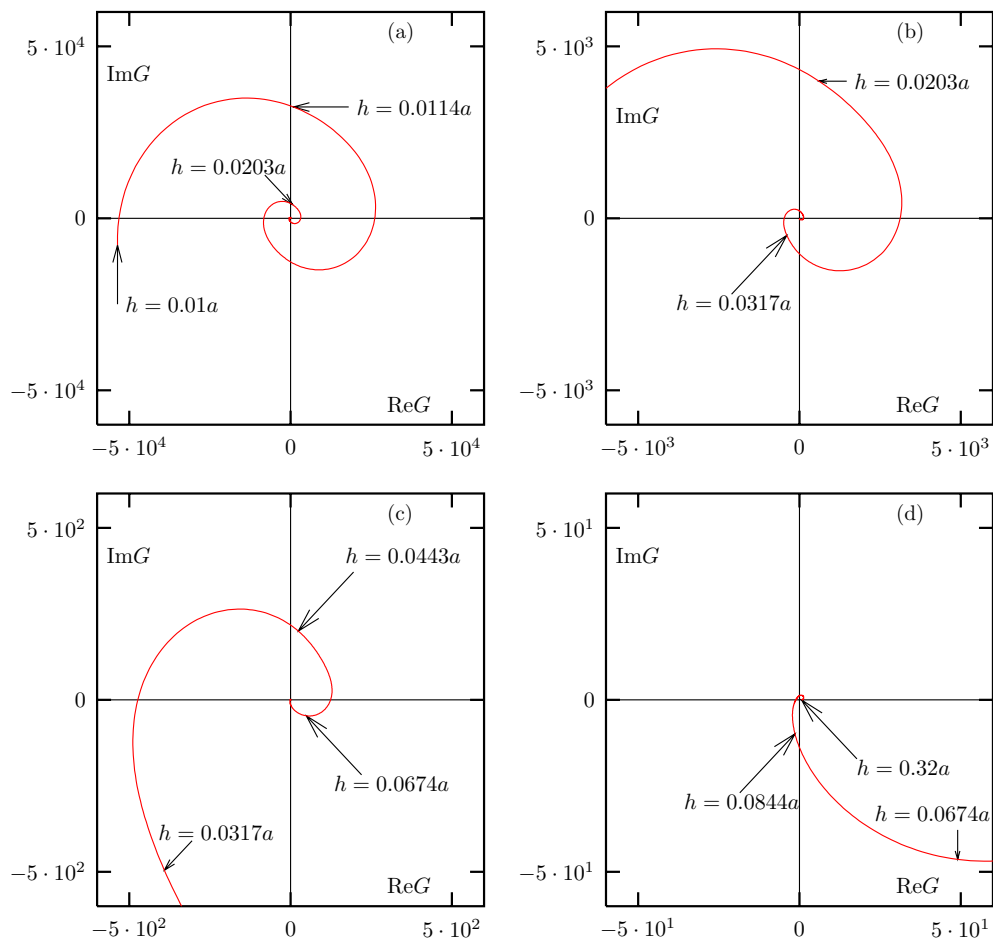


**Figure 5.** Same as in figure 3 but for  $\omega = 0.32\omega_p$ .

On the other hand, the physical effect described in this letter does not originate due to any of the approximations listed above. Instead, it is explained by the resonant nature of the interaction between the electromagnetic field and the nanosystem. When the spacing between the nanospheres is tuned, different resonance modes are excited in the bisphere aggregate. This results the change of the relative phase between the local field in the gap  $E_z$  and the external field  $E_0$  and the characteristic dependence of the enhancement factor  $G$  on  $h$  which is illustrated in figures 3–5. Since the resonance nature of interaction is not altered by the factors mentioned above, it is reasonable to expect that the fine tuning of the third-order nonlinear response is achievable in nanosystems specifically engineered for that purpose.

## References

- [1] Henneberger F, Schmitt-Rink S and Gobel E O 1993 (ed) *Optics of Semiconductor Nanostructures* (Berlin: Akademie Verlag)
- [2] Kreibig U and Vollmer M 1995 *Optical Properties of Metal Clusters* (Berlin: Springer)



- 
- [3] Gaponenko S V 1998 *Optical Properties of Semiconductor Nanocrystals* (Cambridge: Cambridge University Press)
- [4] Shalaev V M (ed) 2002 *Optical Properties of Nanostructured Random Media* (Berlin: Springer)
- [5] Kelly L K, Coronado E, Zhao L L and Schatz G C 2003 *J. Phys. Chem. B* **107** 668
- [6] Li K, Stockman M I and Bergman D J 2003 *Phys. Rev. Lett.* **91** 227402
- [7] Bliokh K Y, Bliokh Y P and Freilikher V D 2004 *J. Opt. Soc. Am. B* **21** 113
- [8] Zou S and Schatz G C 2005 *Chem. Phys. Lett.* **403** 62
- [9] Nordlander P *et al* 2004 *Nano Lett.* **4** 899
- [10] Kneipp K *et al* 1997 *Phys. Rev. Lett.* **78** 1667
- [11] Jiang J, Bosnick K, Maillard M and Brus L 2003 *J. Phys. Chem. B* **107** 9964
- [12] Imoto N, Haus H A and Yamamoto Y 1985 *Phys. Rev. A* **32** 2287
- [13] Shirasaki M and Haus H A 1991 *J. Opt. Soc. Am. B* **8** 681
- [14] Grangier P, Levenson J A and Poizat J-P 1998 *Nature* **396** 537
- [15] Chen Q, Sargent E H, Leclerc N and Attias A-J 2003 *Appl. Opt.* **42** 7235
- [16] Stegeman G I 2001 All-optical switching *Handbook of Optics IV* ed M Bass, J M Enoch, E W V Stryland and W L Wolfe (New York: McGraw-Hill) chapter 21
- [17] Markel V A *et al* 2004 *Phys. Rev. B* **70** 054202
- [18] Gerardy J M and Ausloos M 1980 *Phys. Rev. B* **22** 4950
- [19] Mackowski D W 1995 *Appl. Opt.* **34** 3535
- [20] Markel V A 1995 *J. Opt. Soc. Am. B* **12** 1783
- [21] Markel V A and Poliakov E Y 1997 *Phil. Mag. B* **76** 895
- [22] Stockman M I, Faleev S V and Bergman D J 2001 *Phys. Rev. Lett.* **87** 167401